



Traveling ionosphere disturbances excited ahead of the Tohoku-Oki tsunami: a case study

E. Alam Kherani, L. Rolland, Philippe Lognonne, A. Sladen and Eurico R.de Paula
INPE SJC, Brazil/IPGP, France/GeoAzur, France

Copyright 2015, SBGf - Sociedade Brasileira de Geofísica

This paper was prepared for presentation at the 14th International Congress of the Brazilian Geophysical Society, held in Rio de Janeiro, Brazil, August 3-7 2015.

Contents of this paper were reviewed by the Technical Committee of the 14th International Congress of The Brazilian Geophysical Society and do not necessarily represent any position of the SBGf, its officers or members. Electronic reproduction or storage of any part of this paper for commercial purposes without the written consent of The Brazilian Geophysical Society is prohibited.

Abstract

We document two kinds of traveling ionospheric disturbances, namely, CTIDs (Co-tsunami-Traveling-Ionospheric-disturbances) and ETIDs (Early-Arrival-than-Tsunami-Traveling-Ionospheric-disturbances) related to the Tohoku-Oki tsunami of 11 March 2011. They are, respectively, referred to the disturbances that remain behind and ahead of the principal tsunami wave-front. We first note their presence in a numerical experiment performed using a simulation code coupling the tsunami, atmosphere and ionosphere. This code uses the tsunami wave-field as an input and simulates Acoustic-Gravity Waves (AGWs) in the atmosphere and TIDs, in the form of total electron content (TEC) disturbance, in the ionosphere. The simulated TEC reveals the excitation of CTIDs (at about 2 TECU) and ETIDs (at about 1 TECU), representing up to 5% disturbance over the ambient electron density, and they arise from the dissipation of the AGWs in the thermosphere. A novel outcome is that the strong ETIDs are excited about 20-60 minutes earlier (than the tsunami arrival time) at a location which is about 3°-10° ahead of the instantaneous location of the principal tsunami wave-front. Simulation results are compared with the far-field observations using GNSS satellites and in both, ETIDs are identified as the secondary TEC maximum, occurring 20-40 minutes before the tsunami arrival while the primary TEC maximum representing the CTIDs occurs 10-45 minutes after the tsunami arrival. The ETIDs reported in this study are a new kind of TIDs whose characteristics can be potentially used for the early warning of the tsunami.

Introduction

For this tsunami, number of studies report detailed features of the TEC disturbances or Co-Tsunami-TIDs (CTIDs) excited behind the principal tsunami wave-front [Rolland et al, 2011; Astafyeva et al, 2011; Galvan et al, 2012]. These features include the excitation of near-field elongated elliptical and far-field circular wave-fronts that are propagating with a wide range of phase velocities covering the velocities of the acoustic to gravity waves. Based on Tsunami-Atmosphere-Ionosphere (TAI) coupling through dissipative Acoustic-Gravity waves

(AGWs), numerical simulations of these CTIDs are also presented [Matsumura et al, 2011; Kherani et al, 2012].

In their study, Kherani et al [2012] focused on the study of CTIDs though the study also revealed the presence of another kind of TIDs which we now refer to as ETIDs (Earlier-arriving-than-tsunami-Traveling-Ionospheric-disturbances). The present work aims to investigate the dynamics of these ETIDs based on simulation and observations. Under the present Tsunami-Atmosphere-Ionosphere (TAI) simulation, we examine two scenarios: a pure secondary gravity waves (GWs) scenario and a complete secondary AGWs scenario. These two comparative scenarios are chosen to investigate diverse effects of secondary GWs/AGWs to excite different kinds of TIDs. In particular, we explore a possibility that the AGWs scenario, which is the realistic scenario, can generate the ETIDs ahead of the tsunami since their horizontal propagation in the upper thermosphere is faster than the tsunami waves and that of the GWs. We also search for such ETIDs in the GNSS observations of TIDs at the far-field locations.

Tsunami-Atmosphere-Ionosphere Coupled Simulation model

The TAI coupling mechanism is accomplished in three steps: (i) the excitation of tsunami wave during the Tohoku-Oki tsunami, (ii) the excitation of Acoustic-Gravity Waves (AGWs) by the tsunami wave and (iii) the excitation of ionospheric anomalies by AGWs. The hydromagnetic equations in the ionosphere are written as follows [Kherani et al, 2012]:

$$\frac{\partial \vec{u}_s}{\partial t} = \frac{q_s}{m_s} (\vec{E} + \vec{u}_s \times \vec{B}_0) - \nu_s \vec{u}_s + \nu_s \vec{W}', \quad (1)$$

$$\frac{\partial n_s}{\partial t} + \nabla \cdot (n_s \vec{u}_s) = P - L, \quad (2)$$

$$\nabla^2 \vec{E} - \nabla(\nabla \cdot \vec{E}) - \frac{1}{c^2} \frac{\partial^2 \vec{E}}{\partial t^2} - \mu_0 \frac{\partial \vec{J}}{\partial t} = 0, \quad (3)$$

$$\vec{J} = \underline{\sigma} \cdot \vec{E} + \vec{J}_w; \quad \vec{J}_w = e(n_i \vec{u}_i - n_e \vec{u}_e), \quad (4)$$

$$\nabla^2 \vec{B} - \frac{1}{c^2} \frac{\partial^2 \vec{B}}{\partial t^2} = -\mu_0 \nabla \times \vec{J}. \quad (5)$$

Here (n_s, \vec{u}_s) are the number density, velocity of plasma fluid 's' ($s = \text{ions}(i)/\text{electrons}(e)$), $(q_{i,e} = +Ze, -e)$, (\vec{W}) is the amplitudes of AGWs, ν_s is the frequency of collision between species s-to neutral, \vec{B}_0 is the Earth's magnetic field and \vec{J}_w is the ionospheric current density caused by the AGWs, $(\vec{E}, \vec{J}, \vec{B})$ in above equations are the fluctuating electric field, net current and magnetic field in the ionosphere, $\underline{\sigma}$ is the ionospheric conductivity tensor

and ($c = \frac{1}{\sqrt{\mu_0 \epsilon_0}}$) is the speed of light in vacuum. P, L are the production and loss of ions and electrons by photo ionization and chemical reactions. In addition to the wave equation (7), the electric field, \vec{E} , also satisfies the charge neutrality condition given by following equation:

$$\nabla \cdot \vec{J} = 0 \text{ or } \nabla \cdot (\sigma \vec{E} + \vec{J}_w) = 0 \Rightarrow \nabla \cdot \vec{E} = -\sigma^{-1} (\vec{E} \cdot \nabla \sigma + \nabla \cdot \vec{J}_w) . \quad (6)$$

Equations (1-6) form the closed set of equations to study the temporal and spatial variation of AGWs wind \vec{W} , atmospheric density/pressure (ρ, p), ionospheric number density (n), electric field \vec{E} and magnetic field \vec{B} anomalies. The time $t=0$ in the simulation corresponds to the origin time (5:46:23 UT) of the tsunami. At $t=0$, ambient atmosphere and ionosphere (p_0, ρ_0, n_0, v, T) are obtained from SAMI2 model.

Equations (1-6) are solved numerically using finite-difference method in three dimension that is consists of altitude, latitude and longitude. The implicit Crank-Nicholson scheme is employed to perform the time integration leading to the matrix equation that is subsequently solved by the Successive-Over-Relaxation method. The magnetic dipole coordinate system (p, q, ϕ) is adopted where p, q, ϕ represent the coordinates outward normal to the Earth's magnetic field, northward directed parallel to the Earth's magnetic field and azimuth angle (+ve towards west) respectively. The N-S and E-W boundaries of simulation volume are $23 - 50^\circ N$ and $131 - 156^\circ E$ which covers the region of interest. The lower boundary for the atmosphere and ionosphere are chosen to be the ocean surface and 160 km respectively. The upper boundary is chosen to be 600 km for both atmosphere and ionosphere. At the lower boundary i.e. at the ocean surface-atmosphere interface, the outward normal component W_p of the wind \vec{W} is continuous and is equals to W_T for all time where W_T is the output of the tsunami model. The tsunami wave-field, W_T , is obtained using the tsunami model with the time resolution of 1 minutes [Sladen et al, 2010].

Results

Figure 1 shows the simulation results in which, color images or pixmaps represent the latitude-longitude distribution of ΔTEC , at few selected time (as mentioned at the top of each panel). The ΔTEC is the integrated $\Delta n = n(t) - n(t_p)$ between 160-400 km altitudes where $n(t)$ and $n(t_p)$ are the number densities of electrons at current and previous time (the time step $\Delta t = t - t_p = 30$ seconds). In these plots, also superimposed are the instantaneous principal tsunami wave-fronts, represented by the green contours.

From Figure 1, we may note the following characteristics: **(A)** $\Delta\text{TEC} \sim 2\text{TECU}$ are excited behind and in the vicinity of the principal tsunami wave-front, **(B)** $\Delta\text{TEC} \sim 1\text{TECU}$ are excited ahead of the tsunami wave-front that spread up-to $\sim 3^\circ - 10^\circ$ ahead of the instantaneous tsunami wave-front, **(C)** These ΔTEC anomalies have comparatively longer wavelength than that of the anomalies excited behind the tsunami wave-front.

Discussion

The characteristics noted under (A-C) suggest that with the complete secondary AGWs dynamics, highly energetic-rapidly growing CTIDs and ETIDs are excited. The ETIDs

travel horizontally, much faster than the tsunami itself and reaches farther distances, at any given time. We may note from Figure 1 that after 39 minutes, the excited ETIDs with ~ 1 TECU amplitudes, are ahead by $\sim 10^\circ$ from the tsunami principal wave-front. This means that, considering tsunami velocity of order of 250 m/s, the ETIDs arrives 1 hour earlier (than the tsunami itself) at a location which is 10° ahead of the instantaneous tsunami principal wave-front. This is a novel outcome of the present study that classifies ESTID as a potential candidate for the early warning of tsunami if their presence can be verified from the observations.

In the next section, we present a set of observations in which we are able to identify ETIDs when these observations are complemented by the simulation. At this point, we would like to draw attention towards the first observation of tsunamigenic-TIDs from the all-sky imager over a far-field station, Hawaii [Makela et al, 2011] which revealed the presence of TIDs behind and ahead (or early) of the tsunami wave-front. In addition to the various possible mechanisms discussed by Makela et al [2011], the generation mechanism of ETIDs discussed in the present study offers another plausible interpretation for the observed early waves over Hawaii.

Interpreting the observations

Figures 3a-3b, respectively, depict the observed ΔTEC anomalies along the trajectories of two satellites (PRN=12-1098 and PRN=27-CNMR) using GEONET-GPS network. Upper, middle and lower panels in this figure, respectively, present the spatial distribution, temporal variation and corresponding wavelet spectra of ΔTEC . In the middle panels, the vertical lines are drawn at the arrival time of the tsunami at the two satellite locations. In the middle panels for both the satellites, we note two maxima in the ΔTEC anomaly: a N-shaped primary maximum appearing 10-40 minutes after the tsunami arrival and a secondary maximum that begins to appear 60 minutes prior to the tsunami arrival and last for 40 minutes. Based on previous studies of the Tohoku-OkI tsunami and other tsunamis [Rolland et al, 2010; 2011] which report the presence of CTIDs 10-45 minutes after the tsunami arrival, the primary maxima in Figure 2, can be identified as CTIDs. On the other hand, the presence of secondary maxima prior to the tsunami arrival, as noted from Figure 2, are not examined before. The possibility that such maxima are of the tsunamigenic nature, can be confirmed if complemented with the simulation results.

In Figures 4a-4b respectively, the simulated ΔTEC anomaly along the approximate trajectories of satellites, 1098 and CNMR, are shown. Upper and lower panels of 6a and 6b respectively depict the temporal variation of the simulated ΔTEC (represented by the blue curve) and corresponding wavelet spectra (represented by color image). In the upper panels, also plotted are the tsunami wave-field (represented by the green curve) variation along the trajectories while in the lower panels, corresponding wavelet spectra are plotted as green contours. We note that the simulated ΔTEC along the approximate trajectories reveal the presence of N-shaped primary maximum (marked by thick blue color) at 8:00 GMT (for satellite 1098) and 8:30 GMT (for satellite CNMR) respectively such that these maxima appear $\sim 15-50$ minutes after

the time of tsunami arrival. These N-shaped pulses are identified as CTIDs and they have similar attributes as noted for the observed CTIDs in Figure 2.

Interestingly, prior to the tsunami arrival, the simulated Δ TEC anomaly in Figure 3 reveals the presence of a secondary maximum (marked by thick blue color) that appears 20-40 minutes prior to the tsunami arrival at both satellite locations. These maxima can be identified as ETIDs in Figures 3-4 which are propagating ahead of the tsunami wave-front. Similar secondary maxima are noted in the observed Δ TEC in Figure 2 and therefore the observed secondary maxima are of tsunamigenic nature and can be classified as the ETIDs.

If the observed Δ TEC results from Figure 2 are not complemented by the simulation results from Figure 3, then the observed secondary maxima, that appear prior to the tsunami arrival, may be identified as the precursors, leading to a wrong interpretation. These observed secondary maxima are, as the simulation results suggest, spatially ahead of the tsunami, generated by the tsunami itself and therefore, they are not the tsunami precursors.

The wavelet spectra presented in Figures 3-4 reveal that both observed and simulated CTIDs cover the spectral range between 0.5 mHz-2 mHz (or 32 minutes-8 minutes) with the spectral peak at 1 mHz (or 16 minutes). Moreover, the spectrum of the ETIDs mainly resides around 1 mHz and therefore their spectral characteristics are similar to that of the CTIDs. This similarity suggests that similar to the CTIDs, the ESITDs are originated in the thermosphere. However, the CTIDs are horizontally short waves while the ETIDs are horizontally long waves (as noted in Figure 1). Therefore, though the frequencies of both CTIDs and ETIDs are similar, the ETIDs propagate with the velocities faster than the CTIDs owing to their longer wavelength.

Summary

In the present study, we report the simulation and observations of two kinds of TIDs associated with the Tohoku-Oki tsunami. These TIDs are referred as CTIDs and ETIDs which are excited, respectively, behind and ahead of the principal tsunami wave-front.

Two comparative scenarios, representing the excitations of pure secondary Gravity Waves and the excitations of complete secondary Acoustic-Gravity Waves (AGWs), are examined to understand the origin of ETIDs. It is found that the pure secondary Gravity wave scenario only excites the CTIDs ~ 2 TECU. On the other hand, the complete AGWs scenario excites both CTIDs ~ 2 TECU and ETIDs ~ 1 TECU. This realistic scenario brings out a novel feature that the tsunami-triggered atmospheric and ionospheric anomalies cover wider area in the thermosphere and ionosphere than the tsunami itself such that the significant TIDs, in the form of ETIDs, are excited ~ 20 -60 minutes earlier at a location which is 3° - 10° ahead of the instantaneous principal tsunami wave-front location. The study demonstrates the ability of the complete secondary AGWs to give rise the highly energetic-rapid developing strong-ETIDs. These EIDs are generated from the horizontal thrust arising from the

dissipation of the horizontal momentum of AGWs in the thermosphere.

Observations of TIDs along the trajectories of two GNSS satellites are presented and compared with the simulated TIDs. Although there are mismatches between the modeled and observed TIDs, the presence of two maxima, their time of occurrence, waveform and spectral characteristics match reasonably well. In both, the ETIDs are identified as the secondary maxima in the temporal variation of TIDs that appear 20-40 minutes prior to the tsunami arrival.

These ETIDs are a new kind of TIDs that the present simulation study brings forward together with a new set of observations during the Tohoku-Oki tsunami. Their early presence (as early as 60 minutes prior to the tsunami arrival) in the ionosphere at 10° ahead of the tsunami wave-front classifies them as an important observable for the tsunami early warning at the far-field location.

References

1. Astafyeva E., P. Lognonné and L. Rolland, First ionosphere images for the seismic slip of the Tohoku-oki earthquake *Geophys. Res. Lett.*, 2011, DOI:10.1029/2011GL049623.
2. Galvan, D. A., A. Komjathy, M. P. Hickey, P. Stephens, J. Snively, Y. Tony Song, M. D. Butala, and A. J. Mannucci (2012), Ionospheric signatures of Tohoku-Oki tsunami of March 11, 2011: Model comparisons near the epicenter, *Radio Sci.*, 47, RS4003, doi:10.1029/2012RS005023.
3. Kherani E.A., P. Lognonné et al, Modelling of the Total Electronic Content and magnetic field anomalies generated by the 2011 Tohoku-oki tsunami and associated acoustic-gravity waves, *Geophysical Journal International* Volume 191, Issue 3, pages 10491066 DOI: 10.1111/j.1365-246X.2012.05617.x, 2012
4. Matsumura M., A. Saito, T. Iyemori, H. Shinagawa, T. Tsugawa, Y. Otsuka, M. Nishioka and C. H. Chen, Numerical simulations of atmospheric waves excited by the 2011 off the Pacific coast of Tohoku Earthquake, *Earth Planets Space*, doi:10.5047/eps.2011.07.015, 63, 885–889, 2011
5. Rolland, L. M., G. Occhipinti, P. Lognonné, and A. Loevenbruck, Ionospheric gravity waves detected offshore Hawaii after tsunamis, *Geophys. Res. Lett.*, 37, L17101, doi:10.1029/2010GL044479, 2010.
6. Rolland, L.M., P. Lognonné, E. Astafyeva, E. A. Kherani, N. Kobayashi, M. Mann and H. Munekane (2011), The resonant response of the ionosphere imaged after the 2011 Tohoku-Oki earthquake, *Earth Planets Space*, doi:10.5047/eps.2011.06.020.
7. Sladen A., Tavera H., Simons M., Avouac J.P., Konca A.O., Perfettini H. and Cavagnoud R. (2010), Source model of the 2007 Mw 8.0 Pisco, Peru earthquake: Implications for seismogenic behavior of subduction megathrusts, *J. Geophys. Res.: Solid Earth*, 115, B02405, doi: 10.1029/2009JB006429.

Acknowledgments

EAK thanks FAPESP for the grant under process number 2007/00104-0 and INPE for providing research facility.

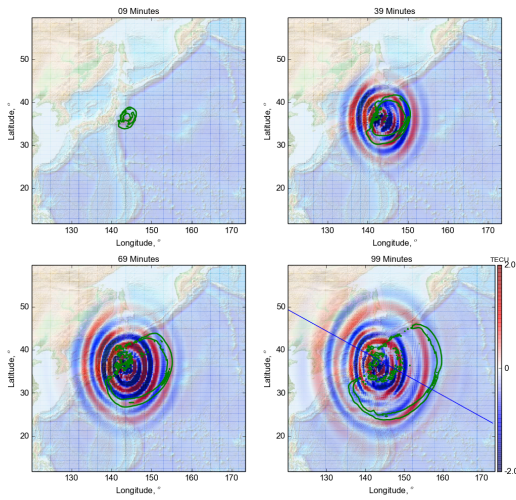


Figure 1: Simulated Δ TEC anomaly: Longitude-latitude distribution of Δ TEC anomaly (represented by the color image or pixmaps) and the principal wave-front of the tsunami wave field W_T (represented by the green contours) are shown at few selected time. The Δ TEC anomalies behind and ahead of the green contour at any given time are defined as the CTIDs and ETIDs respectively.

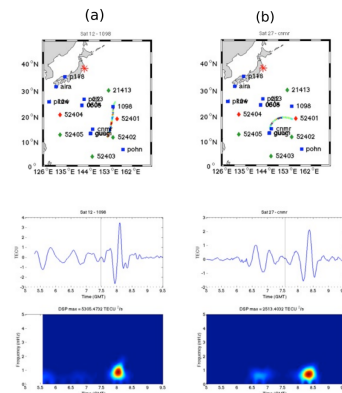


Figure 2: Observed Δ TEC anomaly or TIDs along the trajectories of two GNSS satellites PRN=12-1098 and PRN=27-CNMR in panels (a) and (b) respectively: Spatial distribution (upper panel), temporal variation (middle panel) and corresponding wavelet spectrum (lower panel) are shown. In the upper panels, the epicenter of the tsunami is denoted by the red star and color pixmaps represent the Δ TEC. In the middle panel, the low-pass filtered (less than 5 mHz) data are plotted. The vertical lines in the middle panels are drawn at the arrival time of the tsunami at these satellite locations.

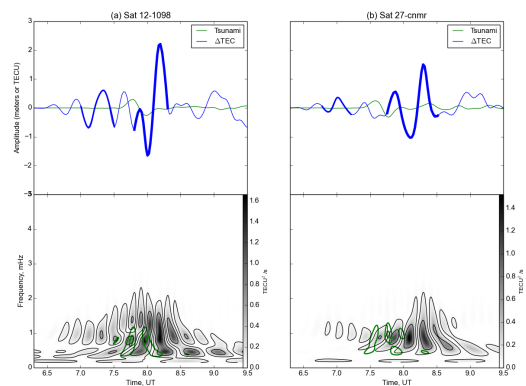


Figure 3: Simulated Δ TEC anomaly or TIDs along the approximate trajectories of two GNSS satellites PRN=12-1098 and PRN=21-CNMR in panels (a) and (b) respectively: In the upper panel, the temporal variation of Δ TEC anomaly and tsunami are shown, represented by blue and green curves, respectively. In the lower panel, corresponding wavelet spectrum of Δ TEC anomaly and tsunami are shown as color image (or pixmaps) and green contours, respectively.